
Photoproduction of η' in quasi-free proton and neutron processes

Collaboration:
F. Huang (UGA)

Part of a combined analysis of

- $\gamma + N \rightarrow M + N$
- $\pi + N \rightarrow M + N$ ($M = \eta, \eta', \omega, \dots$)
- $N + N \rightarrow M + N + N$

(work in progress)

Motivation

- Extract information on nucleon resonances in the less explored higher N^* mass region:
 - high-mass resonances in low partial-wave states.
 - missing resonances.
 - excitation mechanism of these resonances.
- Constrain the $NN\eta'$ coupling constant ($0 \leq g_{NN\eta'} \leq 7.3$):
 - particular interest in connection to the “nucleon-spin crisis” (EMC collaboration, PLB206, '88). $NN\eta'$ coupling constant is related to the flavor-singlet axial charge G_A through the U(1) Goldberger-Treiman relation:

$$2m_N G_A(0) \cong \underbrace{\sqrt{2N_F} F_\pi g_{NN\eta'}(0)}_{\text{quark contribution to the proton “spin”}} + \underbrace{F_\pi^2 m_{\eta'}^2 g_{NNG}(0)}_{\text{gluon contribution to the proton “spin”}}$$

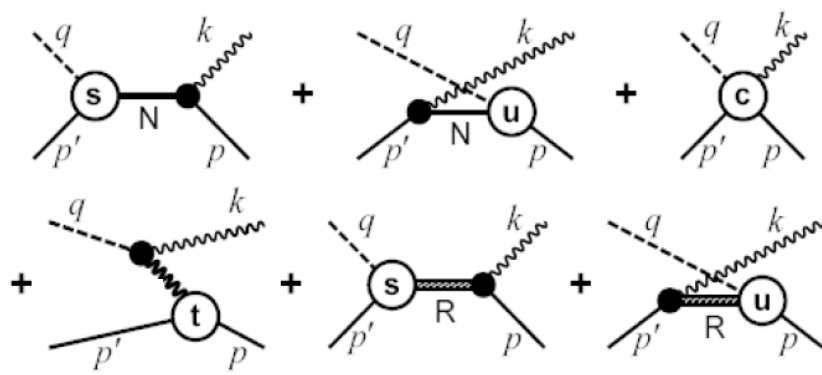
\uparrow

$G_A(0) \approx 0.16 \pm 0.10$
(SMC collaboration,
PRD56, '97)

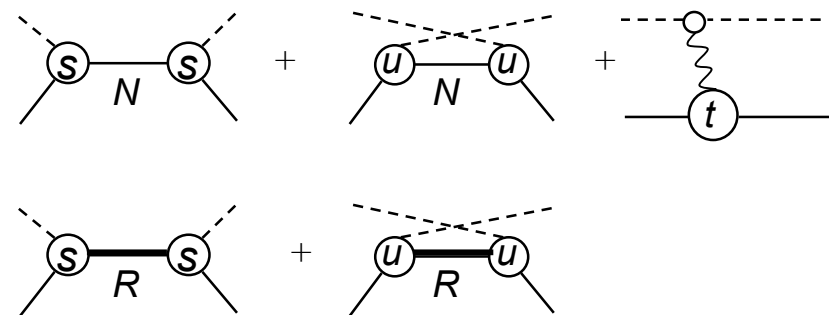
Shore&Veneziano,
NPB381, '92.

Model (for meson production):

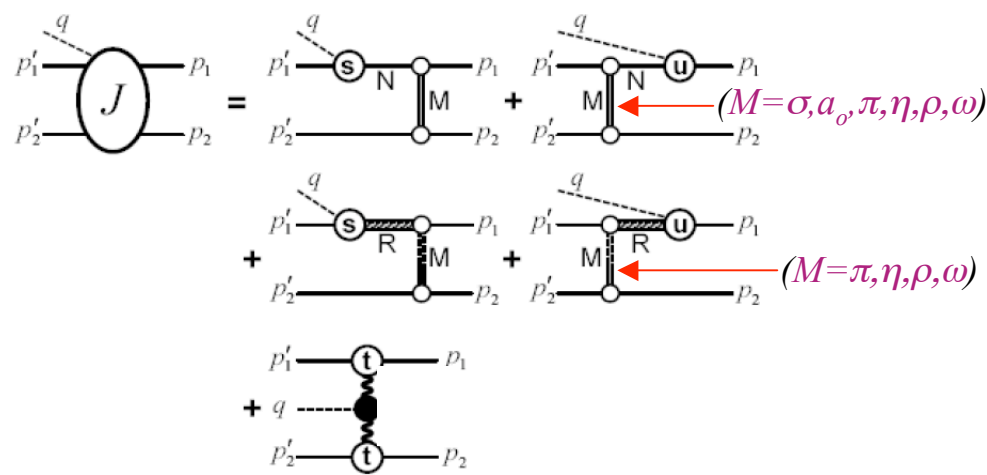
$\gamma + N \rightarrow M + N:$



$\pi + N \rightarrow M + N:$



$N + N \rightarrow M + N + N:$



DWBA:

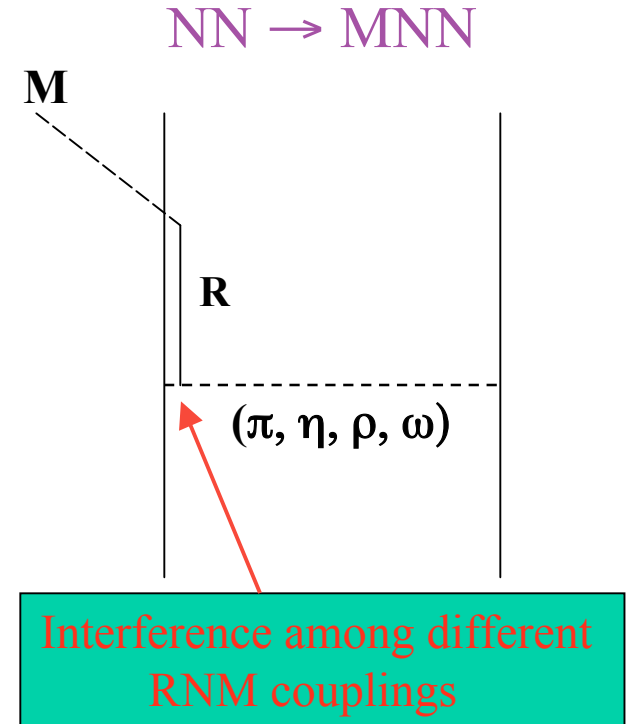
$$A = \underbrace{(1 + T_f G_f)}_{\text{FSI}} J \underbrace{(1 + G_i T_i)}_{\text{ISI}}$$

↑
transition current

Combined analysis of η' production (in the resonance region):

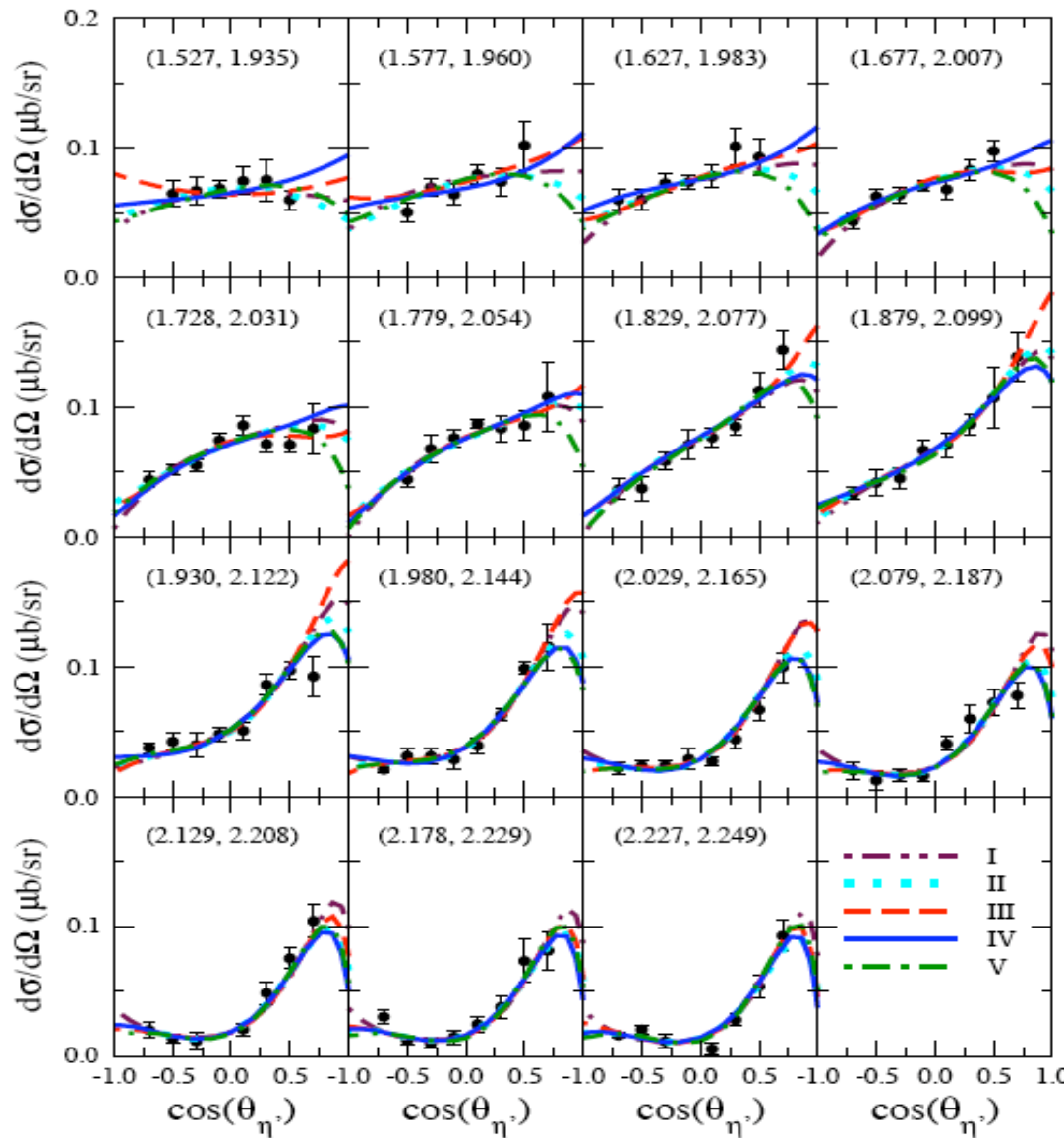
η' meson production :

- $\gamma + N \rightarrow \eta' + N$
 - σ for free proton [ABBHHM, AHHM]
 - $d\sigma/d\Omega$ for free proton [SAPHIR, CLAS, LEPS (available soon)]
 - $d\sigma/d\Omega$ for quasi-free proton & neutron [CBELSA/TAPS (preliminary)]
 - beam asymmetry [CLAS efforts]
- $N + N \rightarrow \eta' + N + N$
 - cross sections for pp [SPECIII, DISTO, COSY-11]
 - cross sections for pn [COSY-11 (preliminary)]
 - pp and pn invariant mass distributions [COSY-11 (P. Klaja, PhD Thesis '09)]



η' photoproduction

$\gamma p \rightarrow \eta' p$: (free proton overview)



- resonances required:
 $S_{11}, P_{11}, P_{13}, D_{13}$
- curves correspond to different set of parameters with comparable fit.
- data at more forward and backward angles would constrain more the model parameters.

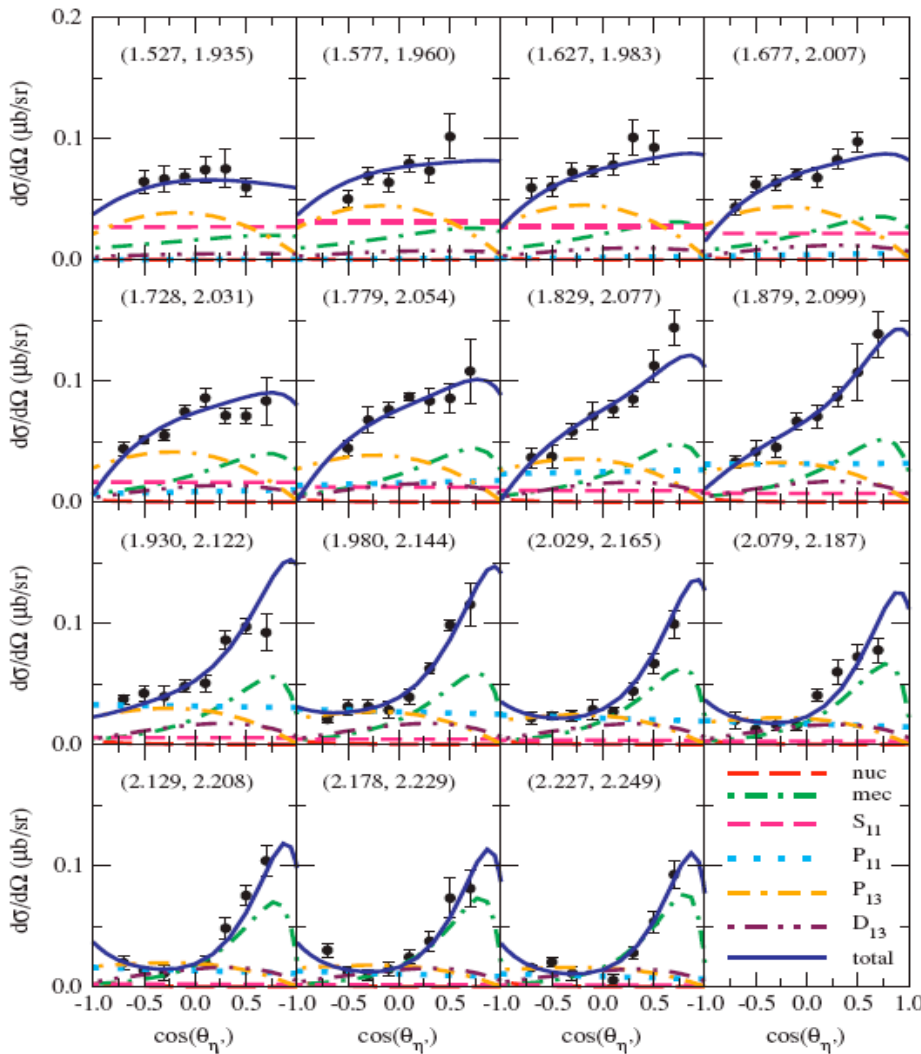
CLAS data:

M. Dugger et al., PRL96, '06

$\gamma p \rightarrow \eta' p$ (dynamical content) :

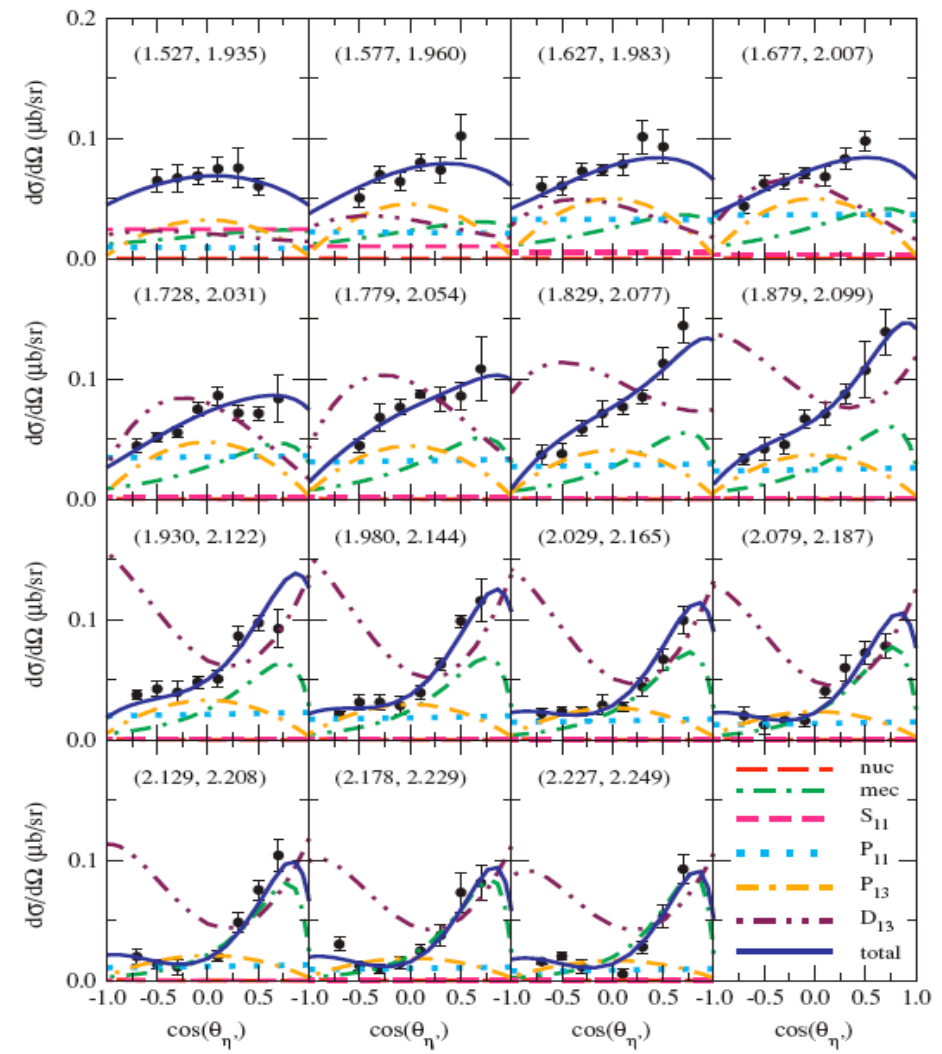
Model I ($\chi^2/N=1.19$) :

$$S_{11}(1958) + P_{11}(2104) + P_{13}(1885) + D_{13}(1823)$$



Model II ($\chi^2/N=1.04$) :

$$S_{11}(1925) + P_{11}(1991) + P_{13}(1907) + D_{13}(1825) + D_{13}(2084)$$



$\gamma p \rightarrow \eta' p$ (can nuc & mec be fixed ?) :

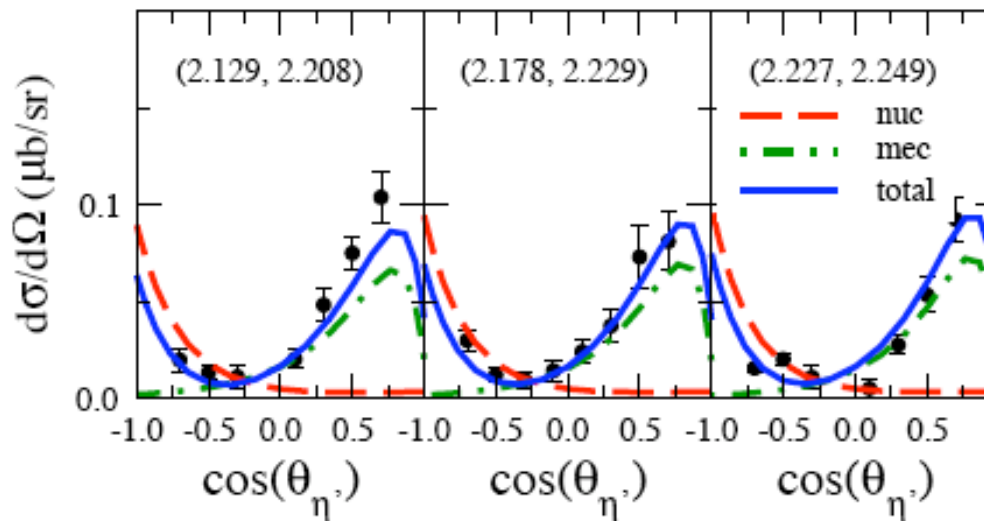
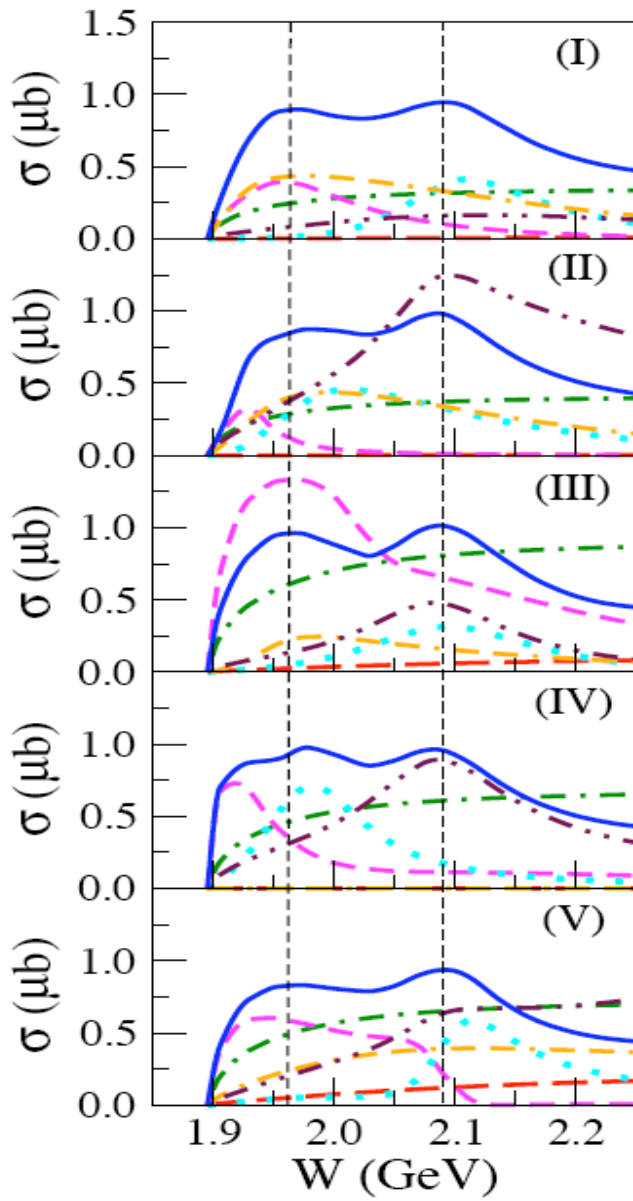


FIG. 9: (Color online) Fit result with no resonances. $g_{NN\eta'} = 2.10$ and $\Lambda_v = 1264$ MeV. See caption of Fig. 4.

would require data beyond the resonance region

$\gamma p \rightarrow \eta' p$ (prediction for the total cross section) :



- sharp rise near threshold due to S_{11} resonance.
- bump around $W=2.09$ GeV due to D_{13} (and possibly P_{11}) resonance.
[PDG: $D_{13}(2080)$ **, $P_{11}(2100)$ *]

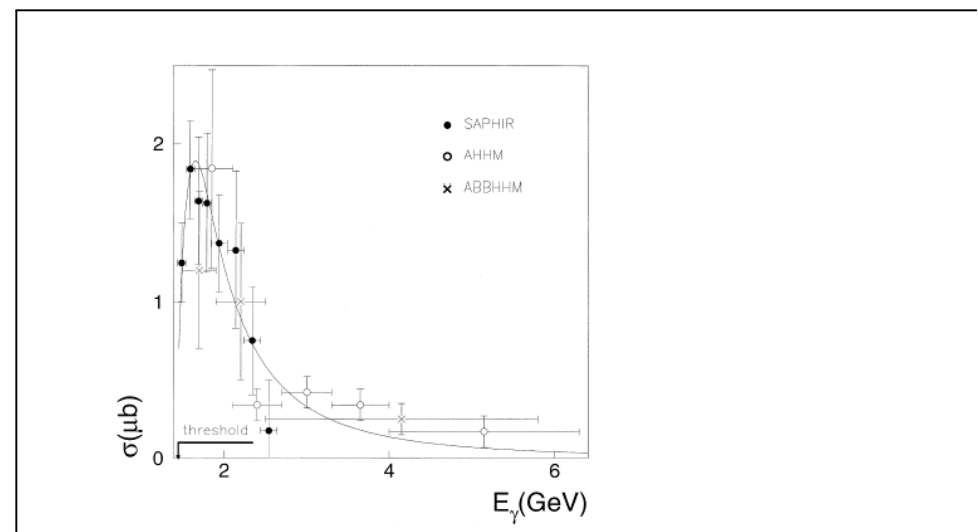
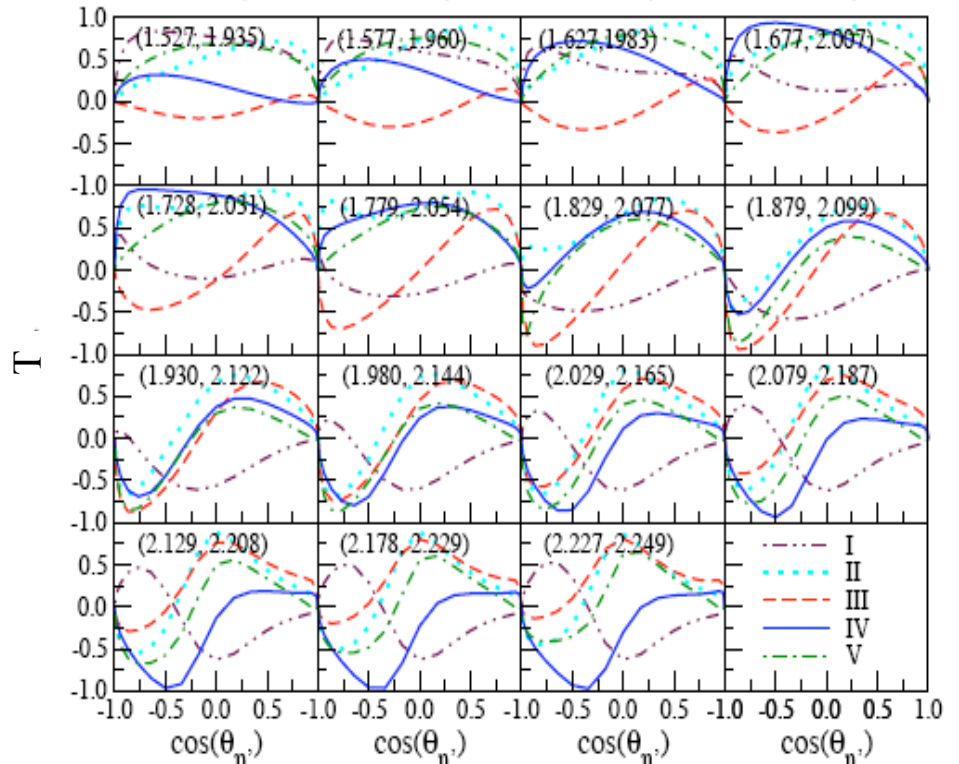
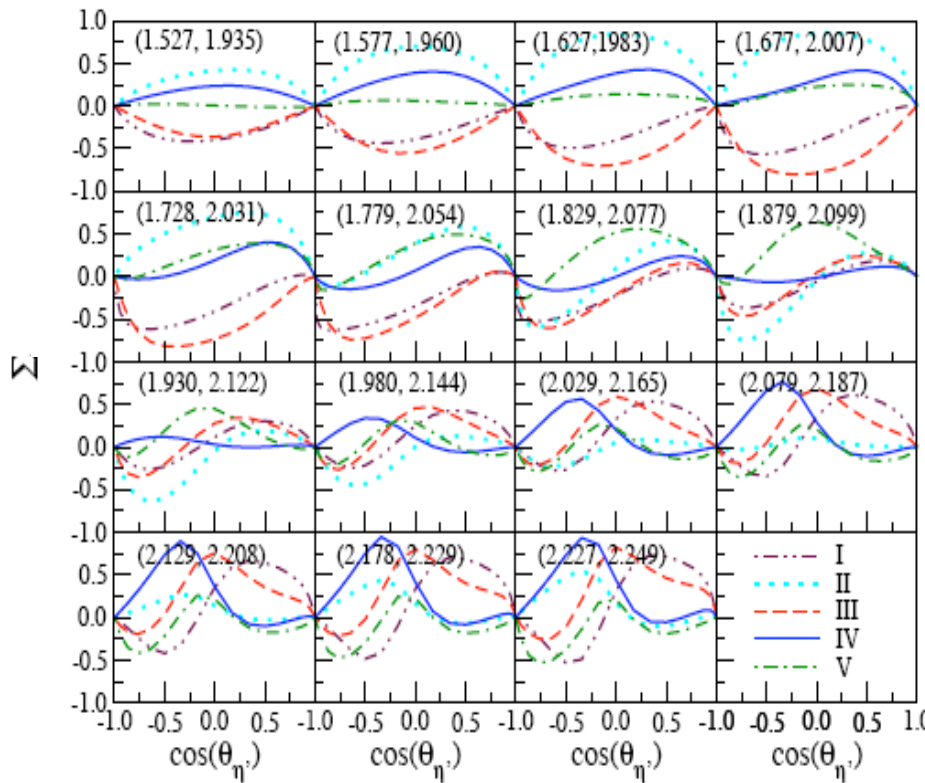


Fig. 4. Measured η' -photoproduction cross section, from this experiment (●), from ABBHHM [1] (×) and from AHHM [2] (○). The solid curve represents the two-resonance fit to the SAPHIR data described below.

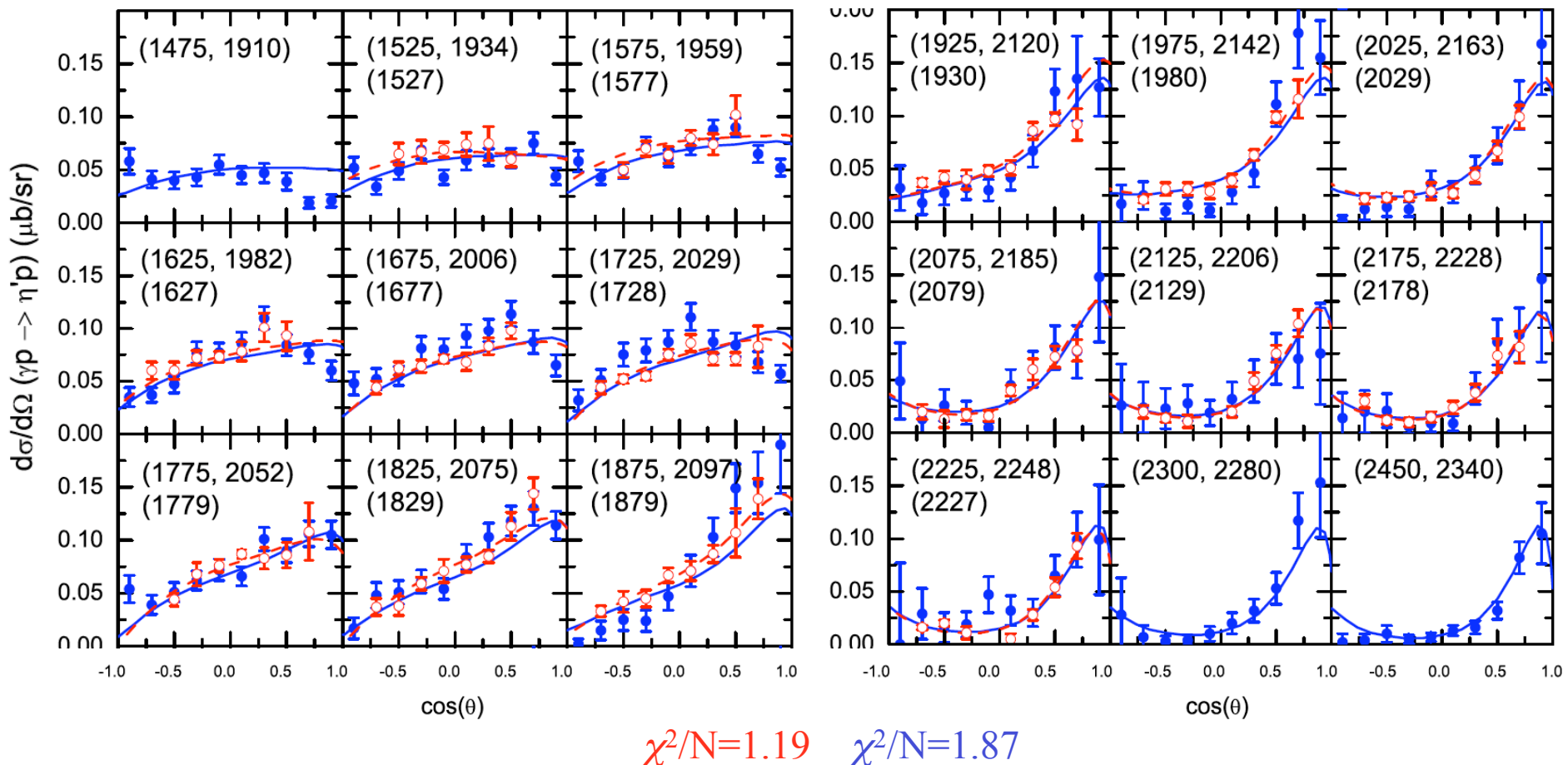
$\gamma p \rightarrow \eta' p$ (beam and target asymmetries) :



much more sensitive to the model parameters than cross sections

CLAS effort: beam asymmetry (M. Dugger et al.)

$\gamma p \rightarrow \eta' p$ (free vrs. quasi-free proton) : model I



Data:

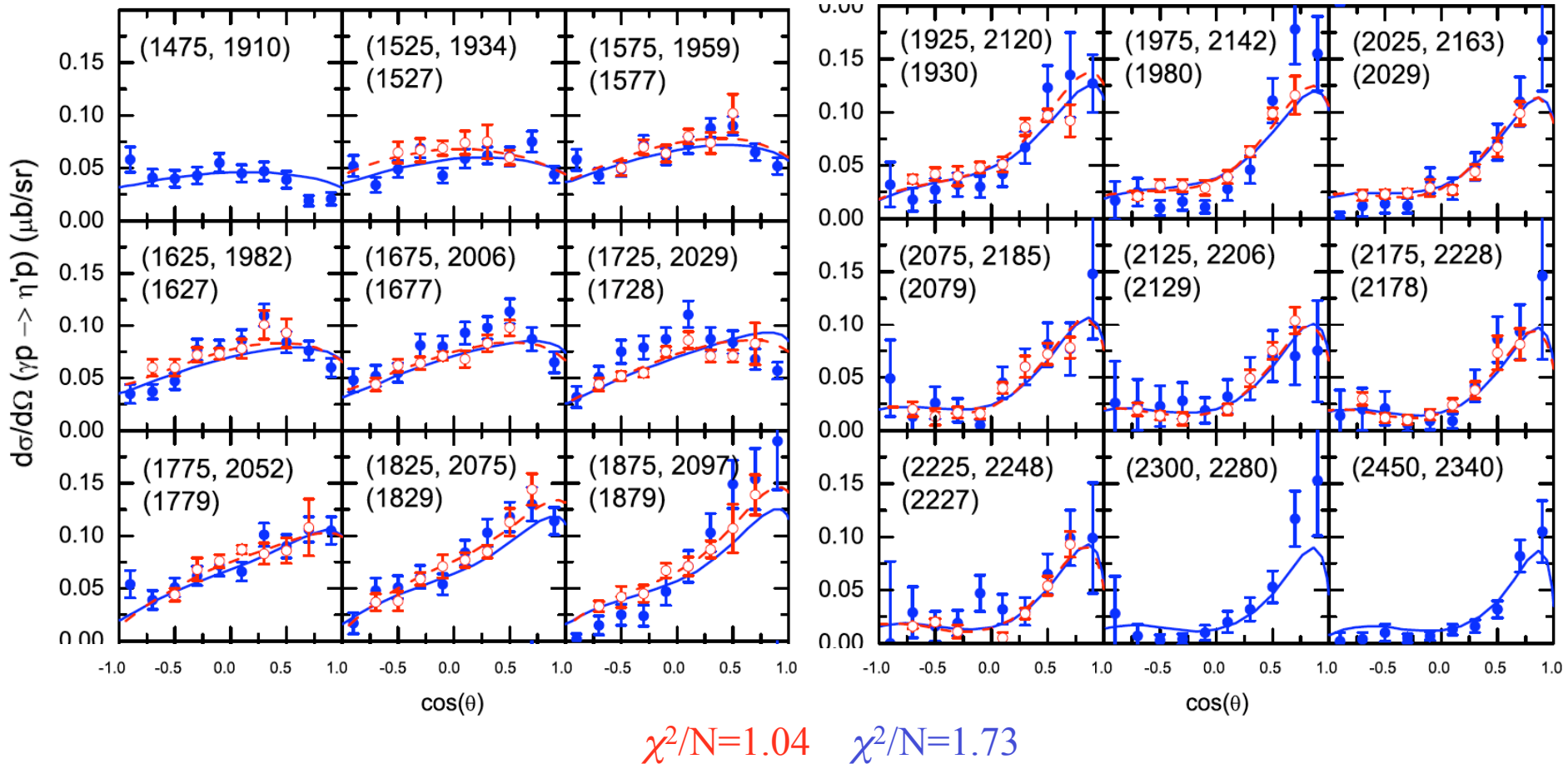
free: CLAS

quasi-free: CBELSA/TAPS (preliminary)

(M. Dugger, et al., PR96, '06)

(I. Jaegle et al., this meeting)

$\gamma p \rightarrow \eta' p$ (free vrs quasi-free proton) : model II



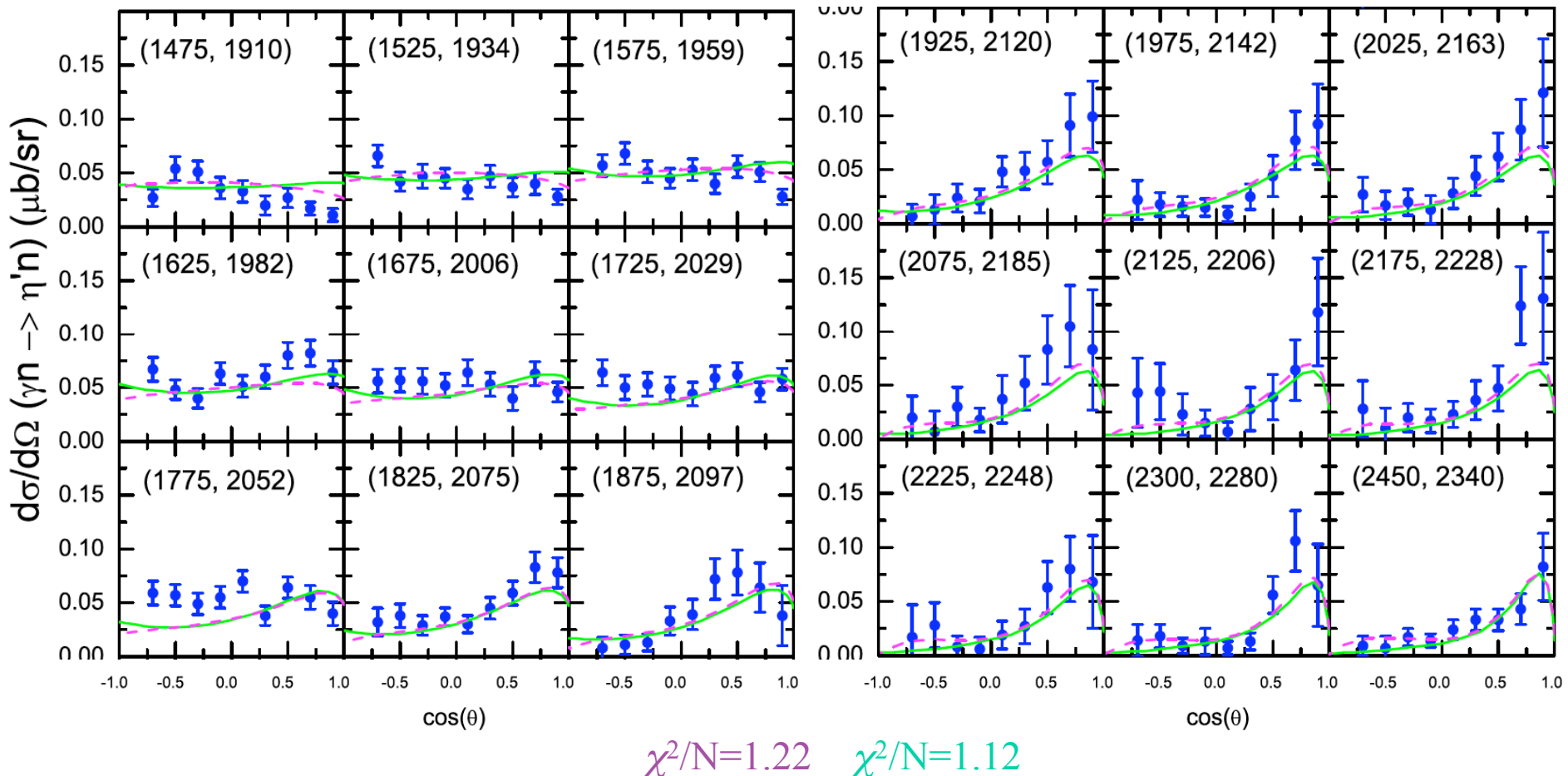
Data:

free: CLAS

(M. Dugger et al., PR96, '06)

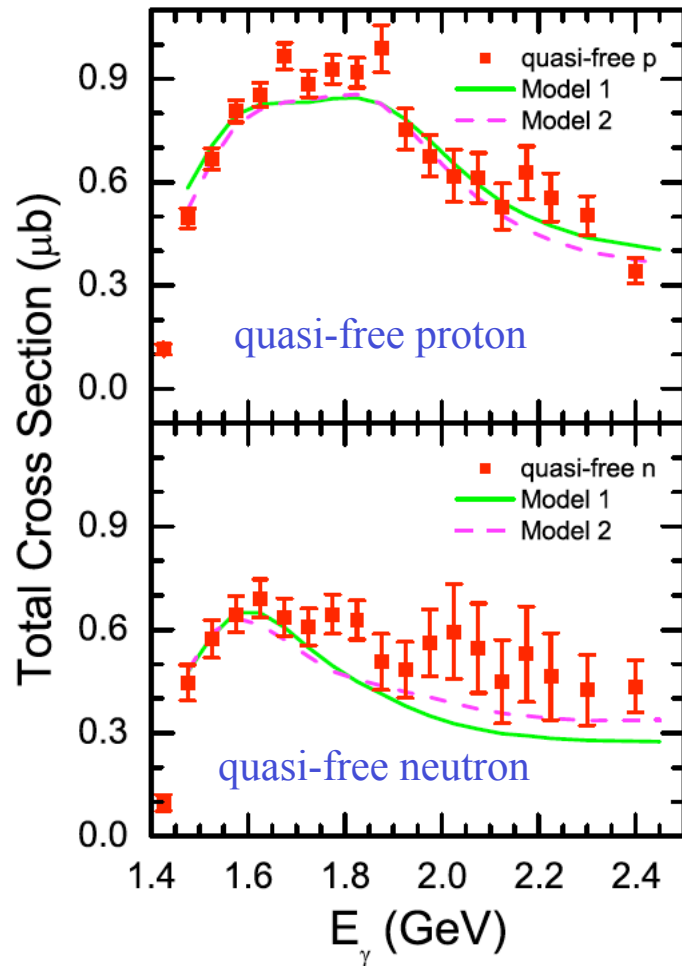
quasi-free: CBELSA/TAPS (preliminary) (I. Jaegle et al., this meeting)

$\gamma n \rightarrow \eta' n$ (quasi-free neutron) : models I & II



Data: CBELSA/TAPS (preliminary) (I. Jaegle et al., this meeting)

$\gamma N \rightarrow \eta' N$ (quasi-free proton vrs neutron)



Model I:

$S_{11}(1958), P_{11}(2104)$
 $P_{13}(1885), D_{13}(1823)$

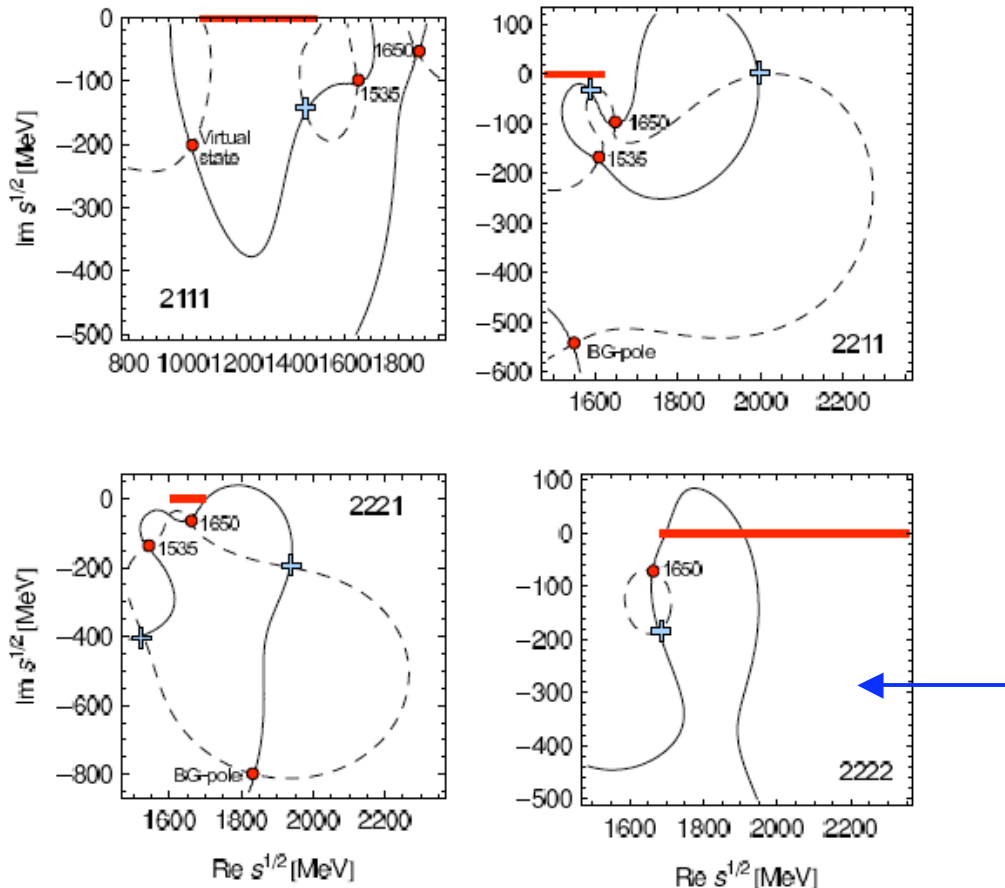
Model II:

$S_{11}(1925), P_{11}(1991)$
 $P_{13}(1907)$
 $D_{13}(1825), D_{13}(2084)$

Data: CBELSA/TAPS (preliminary) (I. Jaegle et al., this meeting)

Remark on sub-threshold resonances:

(M. Doering & K.N.)



$\pi N \quad \eta N \quad K\Lambda \quad K\Sigma$

$x_1 \quad x_2 \quad x_3 \quad x_4$

$x_i = 1$ physical sheet

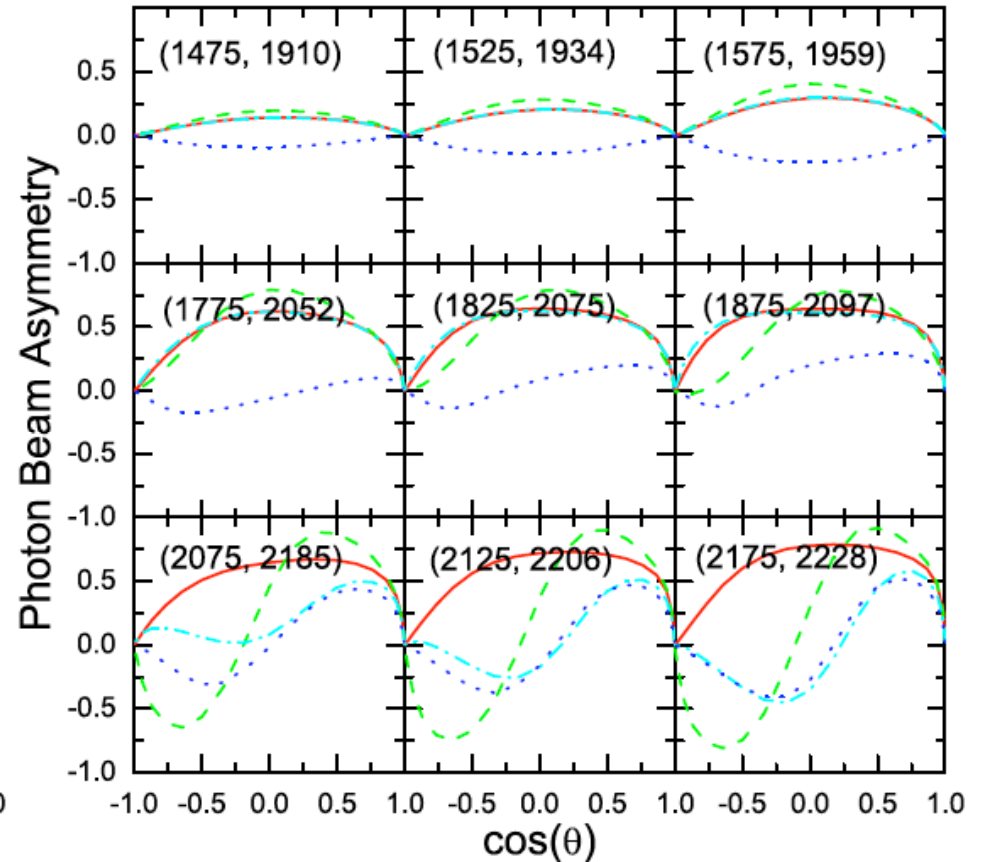
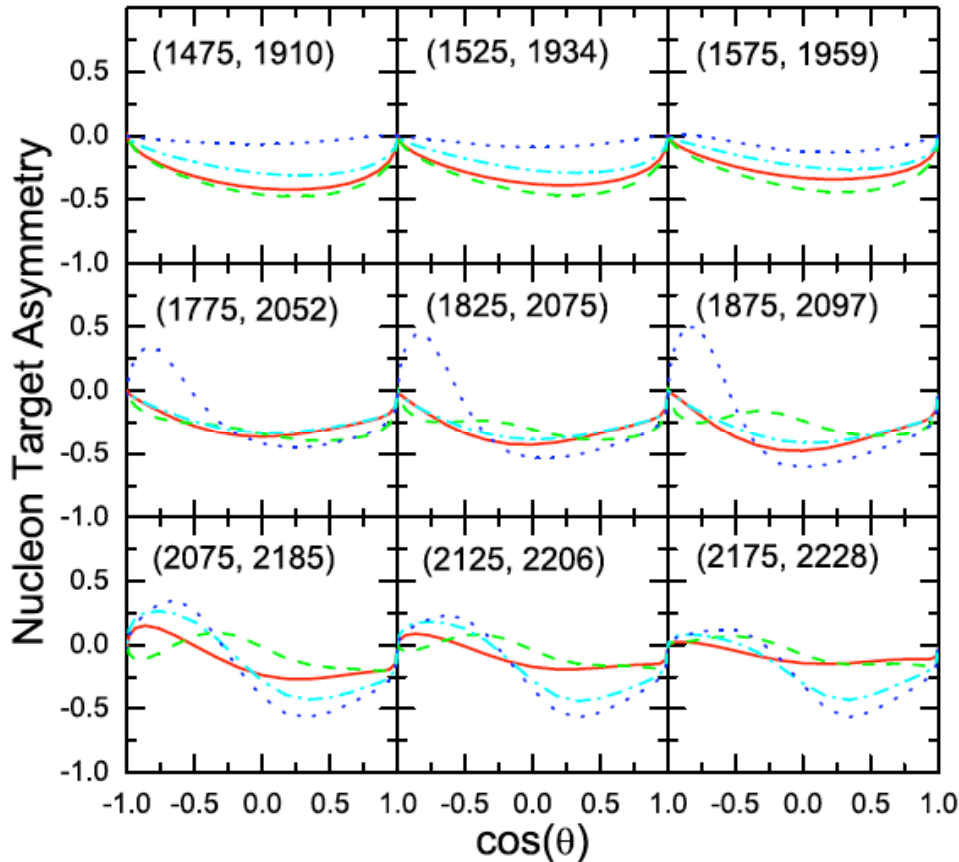
$x_i = 2$ unphysical sheet

Model independent behavior:

if a resonance couples strongly to a given channel the corresponding pole in the unphysical sheet w.r.t. that channel moves far from the physical axis.

FIG. 12: “Gauss plot” of the Riemann sheets 2111 to 2222. The contours $\text{Re } T = 0$ (solid lines) and $\text{Im } T = 0$ (dashed lines) intersect at poles (red circles) and zeros (blue crosses) of the amplitude. The part of the physical axis directly connected to the respective sheet is indicated in bold red.

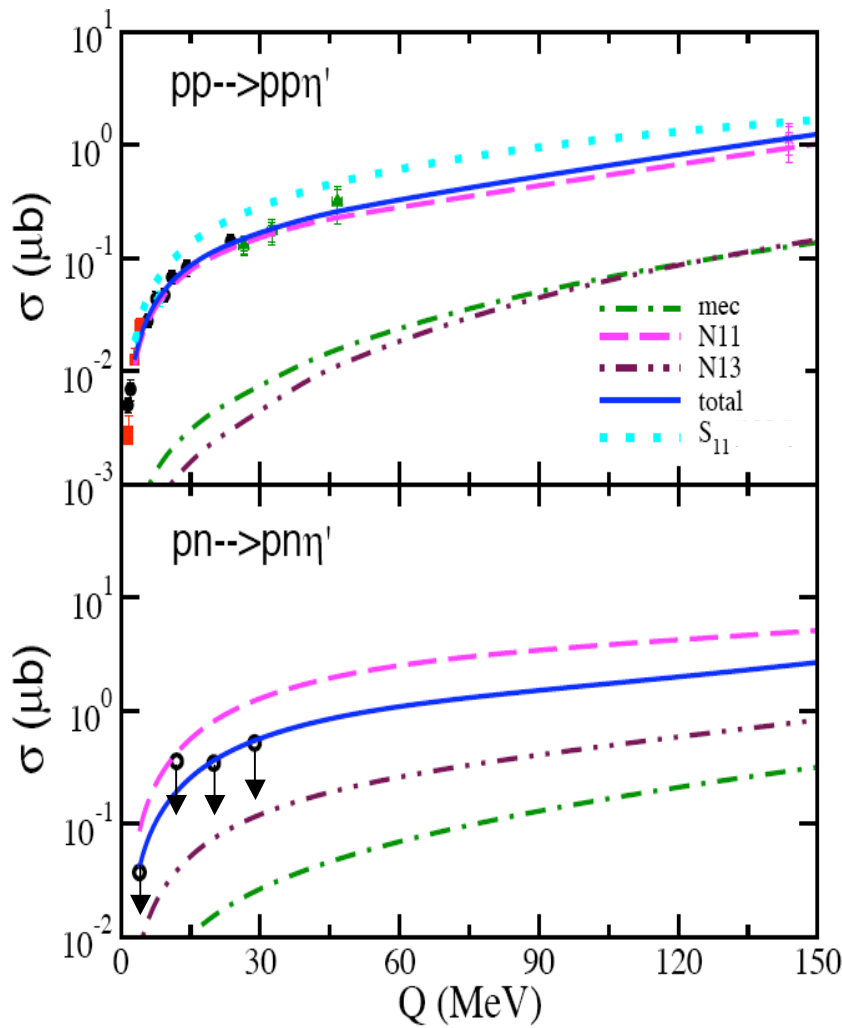
$\gamma p \rightarrow \eta' n$ (quasi-free neutron) : spin-asymmetries



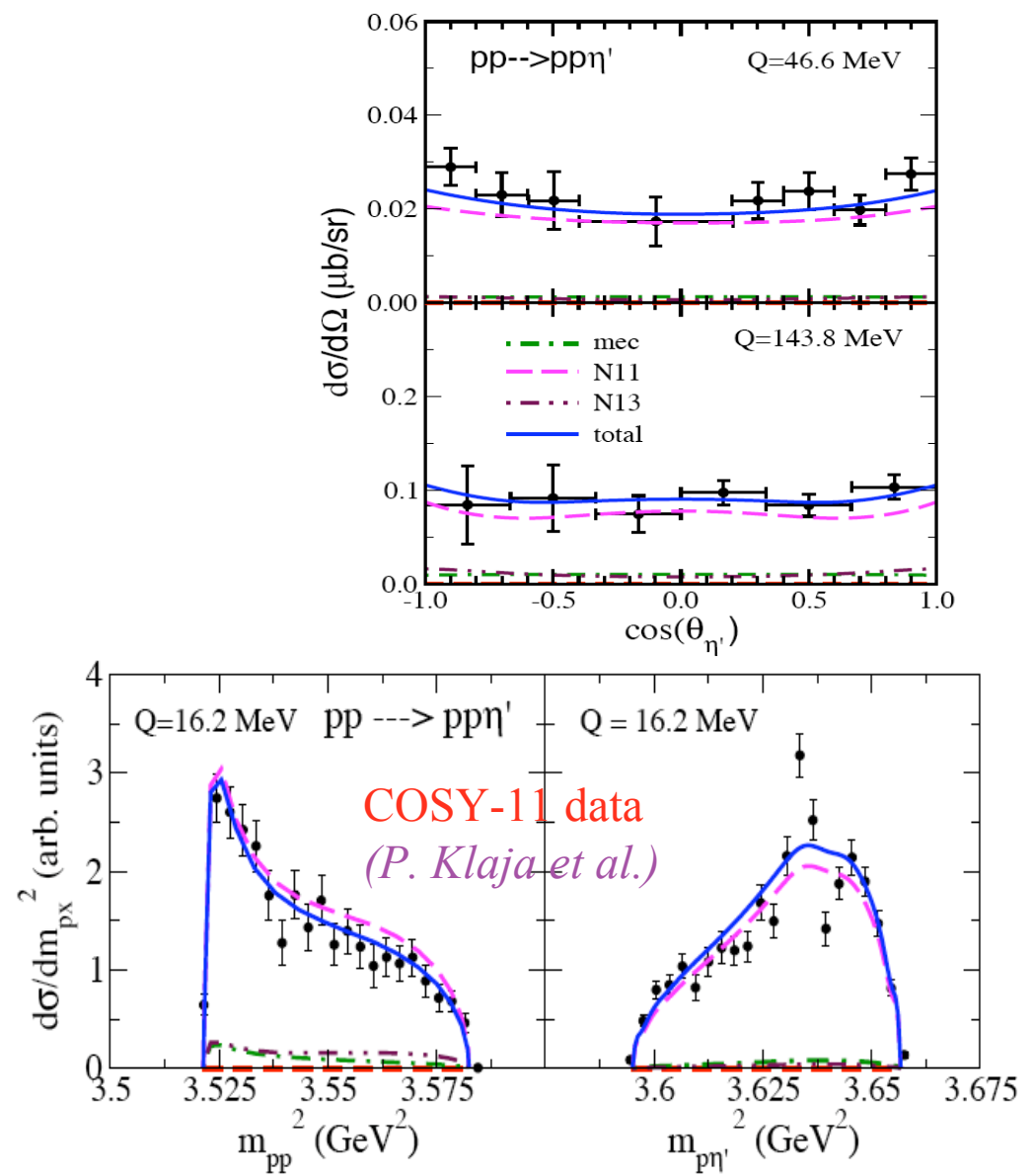
much more sensitive to the model parameters than cross sections



$NN \rightarrow \eta' NN$ (in combination with photoproduction):

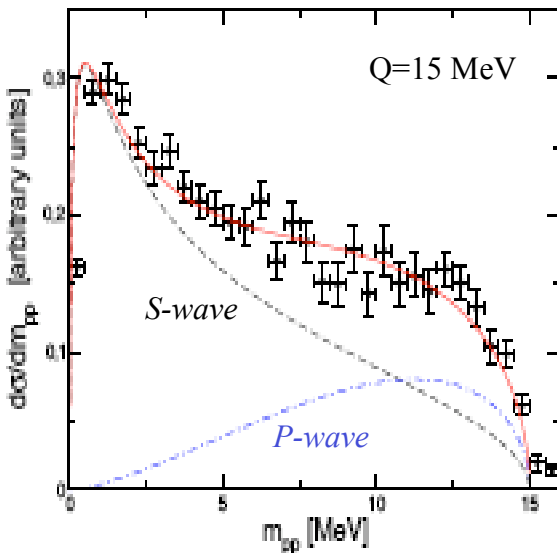


$p\bar{n}\eta'$ prelim. COSY data: (J. Klaja et al.)



COSY-11 data
(P. Klaja et al.)

$NN \rightarrow \eta \ N \ N$: [possible explanation of the pp inv. mass distr.]



(requires an extra p^2 dependence
in the amplitude)

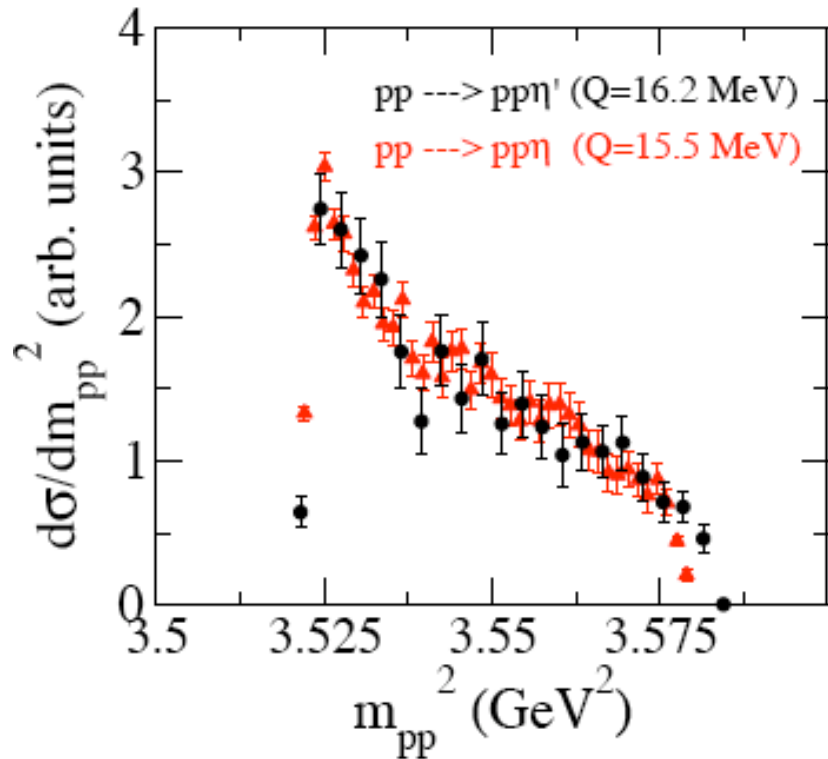
- 1) $p\eta$ FSI & three-body effects (in the S-wave).
(Fix & Arenhövel, PRC'04)
- 2) energy dependence in the (basic) production amplitude.
(Delof, PRC'04)
- 3) higher partial-waves.
(Nakayama et al., PRC'03)

Model independent result (to isolate the S-wave) :

$${}^3\sigma_{\Sigma} = \frac{1}{4}\sigma_o(2 + A_{xx} + A_{yy}),$$

(at threshold: $A_{xx}=A_{yy}=1$) *(Nakayama et al., PRC'03)*

$NN \rightarrow \eta' NN$ (*pp invariant mass distribution comparison with $NN \rightarrow \eta NN$*)



$p\eta'$ FSI is expected to be much weaker than the $p\eta$ FSI.

COSY-11 collaboration data:

$pp\eta$: P. Moskal et al., PRC69, '04.

$pp\eta'$: P. Klaja et al., PhD thesis '09.

Some remarks :

- Resonances are required to describe both the $\gamma + N \rightarrow \eta' + N$ and $N + N \rightarrow \eta' + N + N$ processes.
- (S11, P11, P13, D13) resonances seem to account for the existing data. However, their parameters cannot be determined uniquely from the existing data, especially, their masses are difficult to be fixed since the cross sections show no clear resonance structure. (In this connection, one should be cautious to consider the sub-threshold resonances.)
More exclusive data may reveal more interesting features.
- Spin observables (in particular Σ and T) are definitely required to impose more stringent constraints on the model parameters.

pp- η' pp (some conclusions) :

- Dominant reaction mechanism: S_{11} resonance.
- Existing data cannot constrain on the excitation mechanism(s) of the S_{11} resonance:
 - data on $pn \rightarrow \eta'pn$ and/or $pn \rightarrow \eta'd$ will impose more stringent constraints (isoscalar vrs isovector meson-exchange).
 - and also spin-observables (e.g., A_y in η -meson production can disentangle pseudoscalar- and vector-meson exchanges; also A_{xx}).



The End

Meson exchange currents (mec):

B. Friman, M. Soyeur/Nuclear Physics A 600 (1996) 477–490

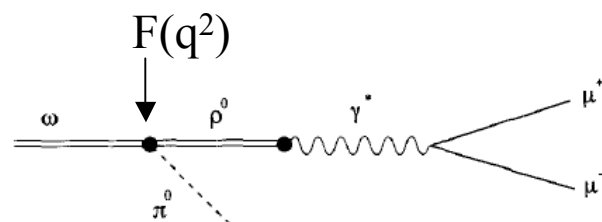


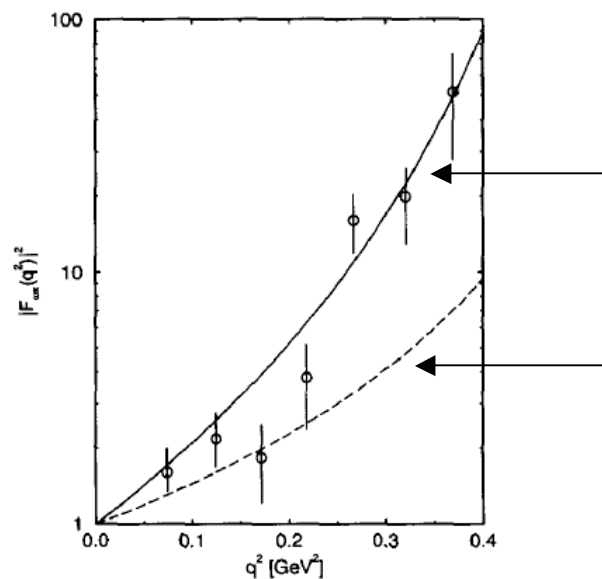
Fig. 3. Vector Dominance Model of the ω Dalitz decay form factor.

we assume for all mec:

$$F(q^2) = \left(\frac{\Lambda_M^2}{\Lambda_M^2 - q^2} \right)^2$$

$$\Lambda_M \sim 1300\text{--}1450 \text{ MeV}$$

$$(\text{not too far from } \Lambda_M \approx \sqrt{2}m_\rho)$$



$$F(q^2) = \frac{\Lambda_M^2}{\Lambda_M^2 - q^2} , \quad \Lambda_M \sim m_\rho$$

$$F(q^2) = 1$$

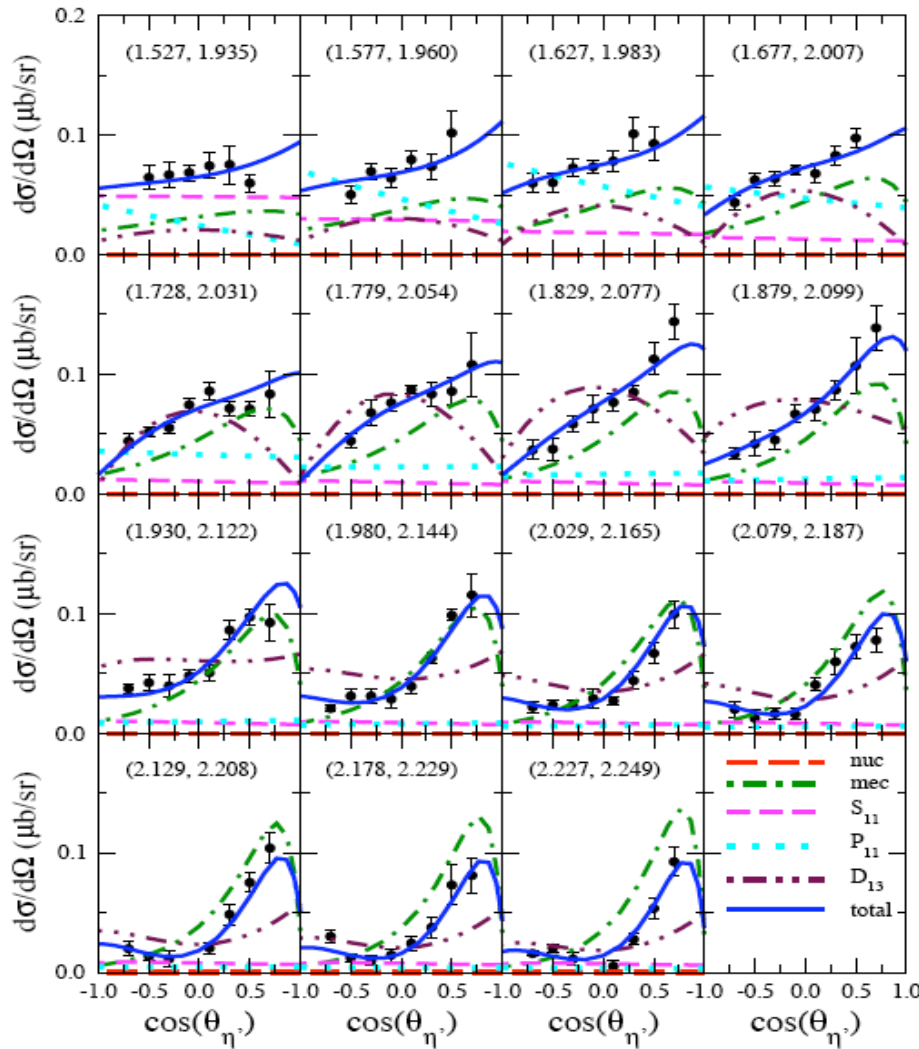
$\gamma p \rightarrow \eta' p$ (model parameters) :

TABLE I: Parameters for Model 1 and Model 2.

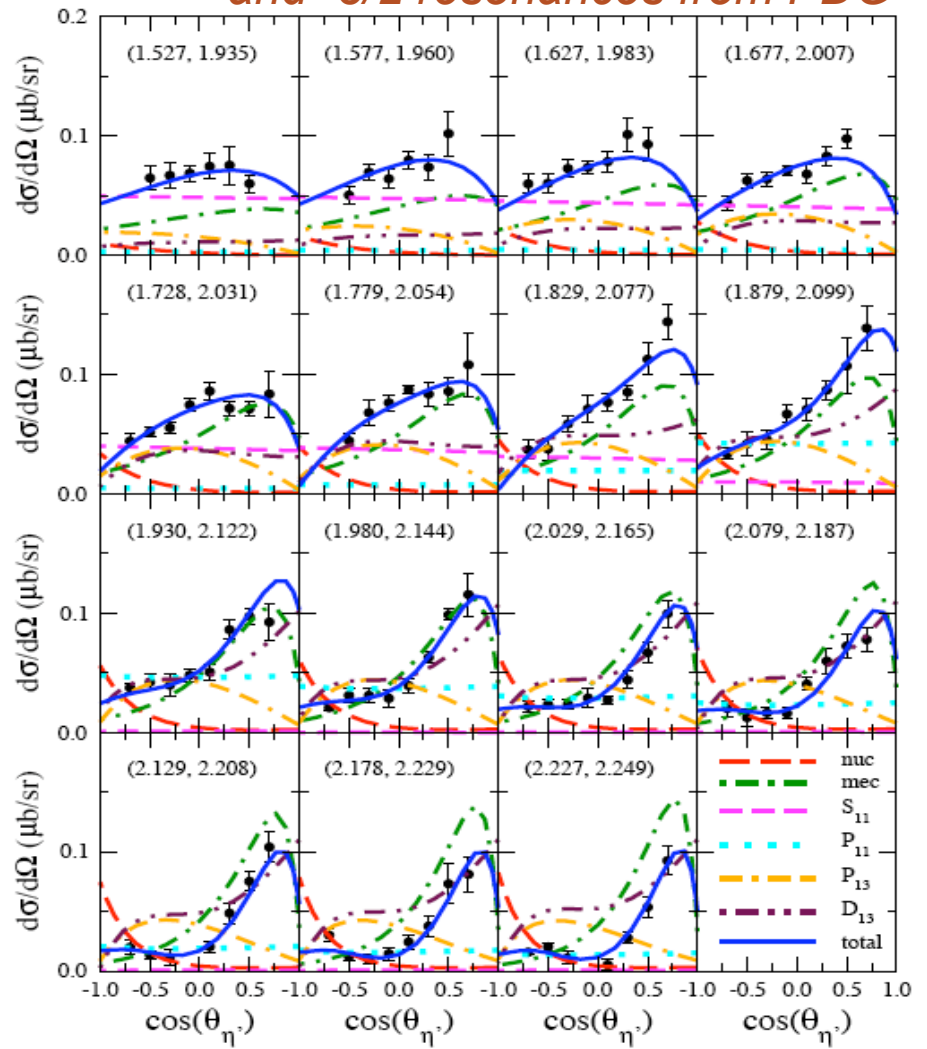
		Model 1 for p (n)	Model 2 for p (n)
S11	M (MeV)	1958	1925
	Γ (MeV)	139	40
	$\gamma_{N\gamma}$	0.0020 (0.0036)	0.0020 (0.0026)
	$\beta_{N\pi}$	0.50	0.56
	$\beta_{N\eta'}$	0.50	0.44
P11	M (MeV)	2104	1991
	Γ (MeV)	136	158
	$\gamma_{N\gamma}$	0.0020 (0.0003)	0.0020 (0.0013)
	$\beta_{N\pi}$	0.36	0.42
	$\beta_{N\eta'}$	0.64	0.58
P13	M (MeV)	1885	1907
	Γ (MeV)	59	123
	$\gamma_{N\gamma}$	0.0020 (0.0000)	0.0020 (0.0012)
	$\beta_{N\pi}$	0.60	0.60
	$\beta_{N\omega}$	0.40	0.40
D13	M (MeV)	1823	1825
	Γ (MeV)	450	55
	$\gamma_{N\gamma}$	0.0020 (0.0000)	0.0020 (0.0000)
	$\beta_{N\pi}$	1.00	1.00
	M (MeV)		2084
	Γ (MeV)		108
	$\gamma_{N\gamma}$		0.0020 (0.0010)
	$\beta_{N\pi}$		0.54
	$\beta_{N\eta'}$		0.46

$\gamma p \rightarrow \eta' p$ (dynamical content) :

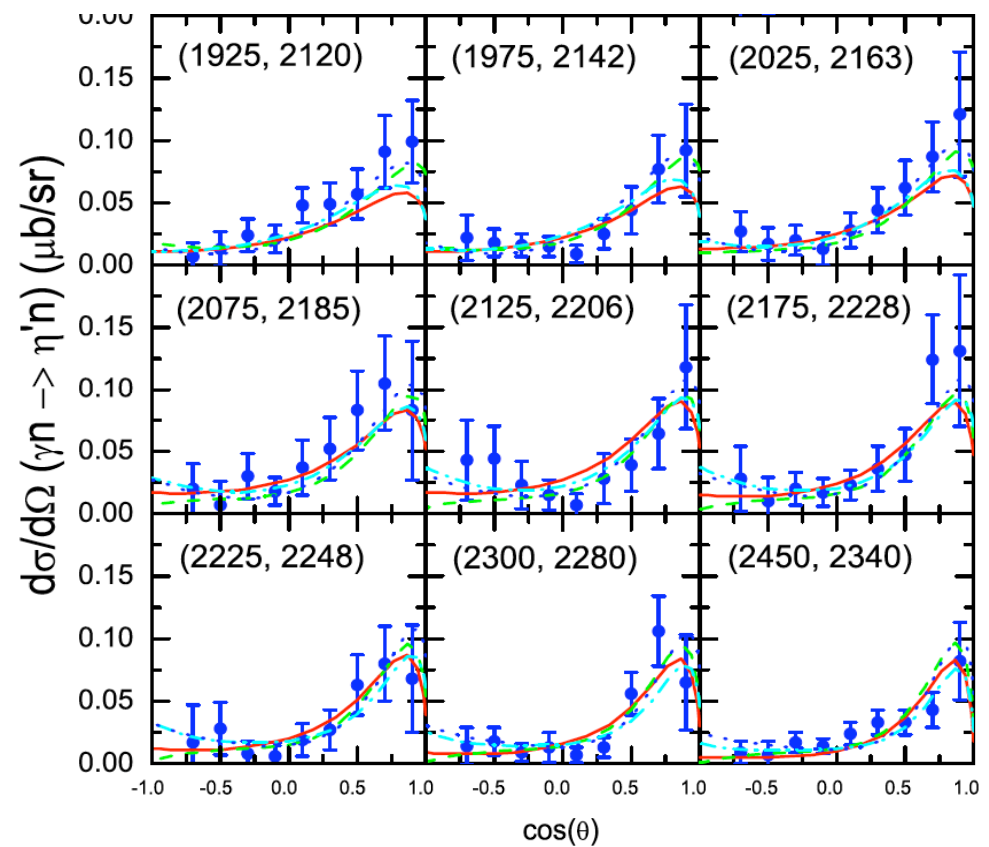
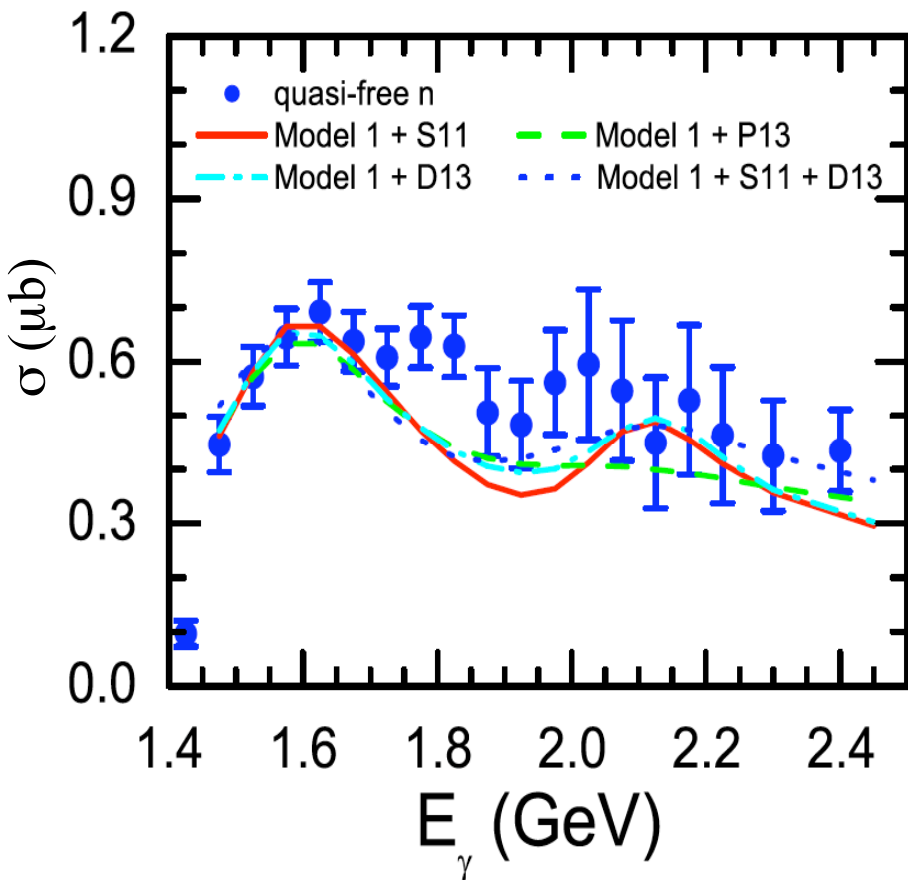
Model IV ($\chi^2=1.10$) : $S_{11}(1535+1848)$
 $+ P_{11}(1710+1996) + D_{13}(1700+2080)$



Model V ($\chi^2=1.01$) : all known spin-1/2
and -3/2 resonances from PDG



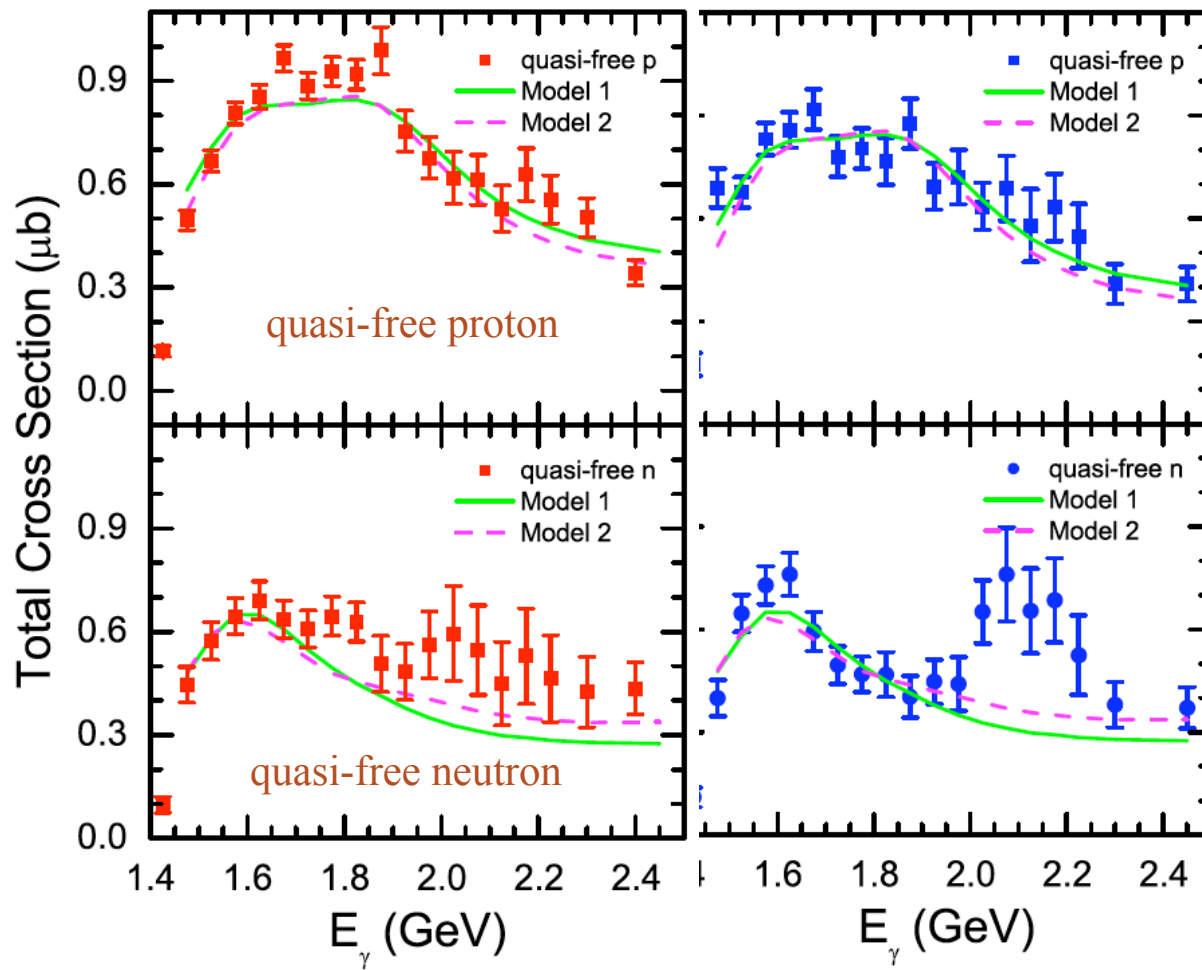
$\gamma n \rightarrow \eta' n$ (quasi-free neutron) : model I + extra resonances



higher-spin resonances are being considered

res.	M_R	Γ_R (MeV)	χ^2/N
S_{11}	2187	45	1.03
D_{13}	2204	50	1.03
P_{13}	2149	179	1.11
$S_{11}+D_{13}$	(2048 , 2191)	(136 , 142)	0.94

$\gamma N \rightarrow \eta' N$ (quasi-free proton vrs neutron)



Model I:

$S_{11}(1958), P_{11}(2104)$
 $P_{13}(1885), D_{13}(1823)$

Model II:

$S_{11}(1925), P_{11}(1991)$
 $P_{13}(1907)$
 $D_{13}(1825), D_{13}(2084)$

Data: CBELSA/TAPS (preliminary) (I. Jaegle et al., this meeting)

$\gamma p \rightarrow \eta' n$: parameter set

II: Parameters fitted to η' photoproduction on quasi-free n based on Model 1 with one or two more additional resonances.

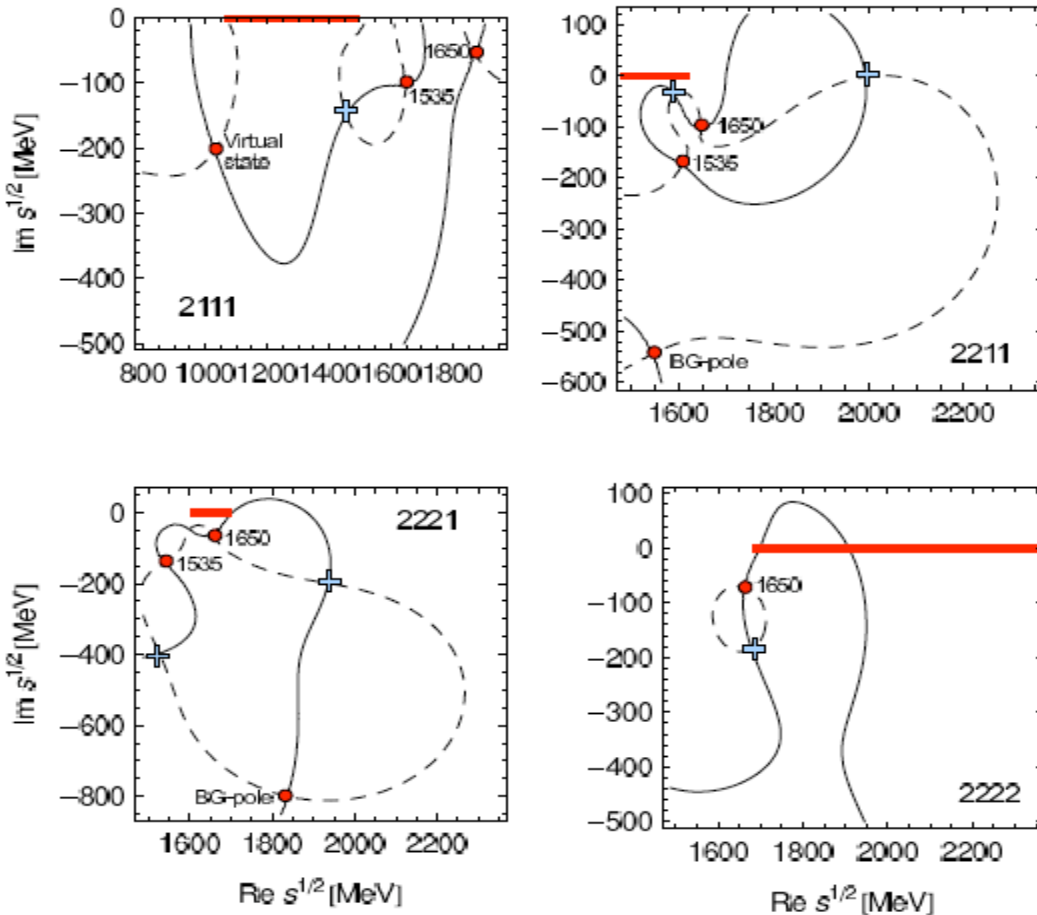
		Model 1 + S11	Model 1 + P13	Model 1 + D13	Model 1 + S11 + D13
S11	M (MeV)	1958	1958	1958	1958
	Γ (MeV)	139	139	139	139
	$\gamma_{N\gamma}$	0.0038	0.0036	0.0039	0.0046
	$\beta_{N\pi}$	0.50	0.50	0.50	0.50
	$\beta_{N\eta'}$	0.50	0.50	0.50	0.50
P11	M (MeV)	2104	2104	2104	2104
	Γ (MeV)	136	136	136	136
	$\gamma_{N\gamma}$	0.0003	0.0003	0.0003	0.0005
	$\beta_{N\pi}$	0.36	0.36	0.36	0.36
	$\beta_{N\eta'}$	0.64	0.64	0.64	0.64
P13	M (MeV)	1885	1885	1885	1885
	Γ (MeV)	59	59	59	59
	$\gamma_{N\gamma}$	0.0000	0.0000	0.0000	0.0000
	$\beta_{N\pi}$	0.60	0.60	0.60	0.60
	$\beta_{N\omega}$	0.40	0.40	0.40	0.40
D13	M (MeV)	1823	1823	1823	1823
	Γ (MeV)	450	450	450	450
	$\gamma_{N\gamma}$	0.0000	0.0000	0.0000	0.0000
	$\beta_{N\pi}$	1.00	1.00	1.00	1.00

$\gamma p \rightarrow \eta' n$: parameter set (cont'.)

S11	M (MeV)	2187	2048
	Γ (MeV)	45	136
	$\gamma_{N\gamma}$	0.0016	0.0019
	$\beta_{N\pi}$	0.02	0.00
	$\beta_{N\eta}$	0.25	0.05
	$\beta_{N\eta'}$	0.73	0.94
P13	M (MeV)	2149	
	Γ (MeV)	179	
	$\gamma_{N\gamma}$	0.0037	
	$\beta_{N\omega}$	0.99	
D13	M (MeV)	2204	2191
	Γ (MeV)	50	142
	$\gamma_{N\gamma}$	0.0099	0.0030
	$\beta_{N\pi}$	0.76	0.00
	$\beta_{N\eta}$	0.00	0.65
	$\beta_{N\eta'}$	0.23	0.35

Sub-threshold resonances?

(M. Doering & K. N.)



($\pi N, \eta N, K\Lambda, K\Sigma$)

x_1, x_2, x_3, x_4

$x_i = 1$ physical sheet

$x_i = 2$ unphysical sheet

FIG. 12: “Gauss plot” of the Riemann sheets 2111 to 2222. The contours $\text{Re } T = 0$ (solid lines) and $\text{Im } T = 0$ (dashed lines) intersect at poles (red circles) and zeros (blue crosses) of the amplitude. The part of the physical axis directly connected to the respective sheet is indicated in bold red.